A novel treatment to enhance survival for end stage triple negative breast cancer using repurposed veterinary anthelmintics combined with gut-supporting/immune enhancing molecules

VIJAYA IRAGAVARAPU-CHARYULU[1], ROJESH SHAKYA[1], PHILIP ROBINSON[2], ESTHER GUZMÁN[3], ANASTASIA TYULMENKOVA[1], JOSE LABRADOR PINO[1] and CEYLAN ISGOR[1]

Departments of [1]Basic Sciences and [2]Clinical Sciences, Charles E. Schmidt College of Medicine, Florida Atlantic University, Boca Raton, FL 33431-0991; [3]Harbor Branch Oceanographic Institute at Florida Atlantic University, 5600 US 1 North, Fort Pierce, FL 34946-7331, USA

Received July 4, 2023; Accepted December 5, 2023

DOI: 10.3892/or.2023.8690

Abstract. Patients with end-stage metastatic disease have limited treatment options and those diagnosed with triple negative breast cancer (Her2, Estrogen receptor, Progesterone receptor) have a poor prognosis. Using a triple negative mammary tumor model selected for brain metastasis (4T1Br4) in the mouse, treatment options that may increase survival when therapeutics are applied at post-metastasis were assessed. Anti-parasitic benzimidazoles (BZs) destabilize microtubules, inhibit metabolic pathways, reduce cell proliferation, and induce apoptosis in tumor cells. Co-administration of two BZs was selected, oxfendazole (OFZ) and parbendazole (PBZ), shown to overcome resistance development in anthelmintic effects by imposing metabolic delay to assess if multiple BZ approach is also suitable to enhance anticancer effects. It has been previously reported that treatment of mammary tumor-bearing mice at an early stage with chitin microparticles (CMPs) decreased tumor growth and metastases by enhancing both innate M1 macrophage and TH1 adaptive immune response. Oral administration of CMPs was previously revealed to affect the gut in intestinal inflammation. A combination BZ (OFZ/PBZ) and CMP treatment was tested to target tumor development and metastasis and effects were compared in response to monotherapies of the same compounds or to untreated mice. The results demonstrated increased survival, decreased tumor cell proliferation, decreased metastasis in lungs and brain, increased levels of fecal SCFAs butyric, acetic, propionic and valeric acids with increased butyric and propionic acid levels in brain biopsies in combination treated compared with untreated mice. At the primary tumor, SCFA receptor FFAR2 expression was increased in combination treatment compared with untreated mice, suggestive of a non-invasive cancer phenotype. The superior cytotoxic effects of OFZ/PBZ were confirmed as opposed to single treatment with OFZ or PBZ using 3D spheroids generated from a human breast cancer cell line, MDA-MB-468. These data are compelling for treatment option possibility even at late stages of metastasized breast cancer.

Introduction

Triple negative breast cancer has higher mortality rate compared with those expressing hormone and/or growth factor receptors with standard treatment options that include mostly neoadjuvant chemotherapy (NACT), surgery and radiation (1,2). Depending on the gene mutation signature of the triple negative tumors, other treatment options to improve prognosis include targeted drugs such as Poly (ADP-ribose) polymerase (PARP) inhibitors or immunotherapies (3,4). Pathologic complete response rate of patients undergoing combination of NACT and immunotherapies if administered early is favorable (5,6). However, the triple negative tumors become chemoresistant and tend to recur more frequently after treatments compared with other breast cancers (7-9). Thus, treatments for advanced triple breast cancer patients have been met with limited success resulting in increased mortality. In the present study, additional treatment options that could offer hope for late-stage cancers were explored.

Previous studies implicate the influence of gut microbiome on breast cancer prognosis. Alterations in gut microbiome promote metastasis and several case control studies have linked dysbiosis to both the initiation of breast cancer and

Correspondence to: Dr Ceylan Isgor or Dr Vijaya Iragavarapu-Charyulu, Department of Basic Sciences, Charles E. Schmidt College of Medicine, Florida Atlantic University, 777 Glades Road, Boca Raton, FL 33431-0991, USA
E-mail: cisgor@health.fau.edu
E-mail: iragavar@health.fau.edu

Abbreviations: BZs, benzimidazoles; CMPs, chitin microparticles; FBZ, fenbendazole; FFAR2, free fatty acid receptor 2; IHC, immunohistochemistry; OFZ, oxfendazole; PBZ, parbendazole; SCFAs, short chain fatty acids

Key words: benzimidazoles, chitin microparticles, metastasis, short chain fatty acids, free fatty acid receptor 2, oxfendazole, parbendazole, breast cancer

enhancing metastasis to the lungs independent of tumor volume (10). Complex carbohydrates are metabolized by commensal gut microbes to produce short chain fatty acids (SCFAs) such as acetate, propionate and butyrate that promote immune responses yet maintain tolerance in the gut (11). While SCFAs have been reported to suppress TH2 responses during helminth infections (11), SCFAs interacting with their receptors, FFAR2, have been identified to promote a non-invasive tumor phenotype and thus hold promise for slowing metastasis (12,13).

Benzimidazoles (BZs) are used to treat parasitic infections in animals and humans and have been also shown to have anticancer effects. *In vitro* treatment of tumor cell lines with fenbendazole (FBZ), a member of BZ compounds resulted in inhibition of cancer cell proliferation (14). Furthermore, previous *in vivo* studies revealed promising anticancer effects with various BZ treatments (15-19). Specifically, BZs and their derivatives were demonstrated to inhibit triple negative breast cancer, glioblastoma and cancers of the digestive system by destabilizing microtubules, inducing cell cycle arrest and apoptosis (17,20,21). BZs have been also shown to inhibit angiogenesis (22), inhibit metabolic pathways, reduce cell proliferation, and induce apoptosis in tumor cell lines (23). In contrast to chemotherapeutics such as taxanes and vinca alkaloids, BZs are more selective in their on-target effects towards rapidly dividing and invasive cells but sparing the healthy host cells (14,24). Taxanes are known to cause cell cycle arrest and apoptosis by interfering with spindle microtubule dynamics (24-26). Vinca alkaloids on the other hand arrest cancer cell growth by binding to mitotic spindle microtubular proteins resulting in crystallization of the microtubular proteins causing either mitotic arrest or cell death (27). However, similar to the conventional chemotherapeutics, resistance to anticancer effects of BZs may develop. For example, a prolonged treatment with FBZ has been observed to develop resistance during anthelmintic treatment (28). To overcome emergence of resistance, co-administration of specific BZs (i.e., oxfendazole, OFZ; and parbendazole, PBZ) that interact to transiently delay metabolism is successfully utilized in anthelmintic applications (29,30). OFZ [methyl (5-(phenylsulphinyl)-1H benzimidazole-2-yl) carbamate] has a long metabolic half-life and is metabolized to FBZ which is also a bioactive BZ (31). Specifically, OFZ is cytotoxic to cancer cells, and induces cell cycle arrest. It has been also found to enhance the cytotoxicity of alkylating agents such as cisplatin (32). PBZ [N-(6-butyl-1H-benzimidazol-2-yl) carbamic acid methyl ester] is a carbamate ester. Specifically, PBZ inhibits cancer cell proliferation, clonogenicity and migration through its adverse effects on microtubule organization and formation. In addition to its effects in mitotic catastrophe, PBZ has been also reported to be a potent apoptotic agent through DNA damage (33). In the present study, this combination of OFZ/PBZ was explored as a potential for a chronic anticancer treatment regimen with sustained efficacy. A previous *in vivo* study by the authors demonstrated that when mammary tumor bearers are treated with chitin microparticles (CMPs), there is decreased tumor growth/metastasis partly due to the effect on production of inflammatory molecules and on $CD4^+$ T helper (TH) cell populations with a shift from TH1, a proinflammatory type with IFN-γ production to TH2, immunosuppressive type with IL-4 production (34). Treatment with FBZ is known to attenuate TH2 response (35). A TH1 immune response with IFN-γ production is crucial for inhibiting tumor progression while TH2 type has been reported to promote tumors (36). Although previous studies by the authors using CMPs to treat murine breast cancer showed a decrease in tumor growth and a significant decrease in metastasis (34,37), the tumors were not completely eradicated. Identifying and prioritizing treatment options for late-stage cancer is critical for prolonging and improving quality of life of breast cancer patients. In the present study, the use of repurposed veterinary drugs (multiple BZs, OFZ/PBZ), either singly or in combination along with CMPs, was investigated as novel treatment options to enhance survival in post metastatic, late-stage breast cancer using an *in vivo* animal model of aggressive breast cancer selected for brain metastasis [4T1Br4] (38). Two BZs (i.e., OFZ and PBZ) were specifically selected; when co-administered, they potentiate each other's therapeutic effects and remain bioactive for longer period of times in the blood stream due to delayed hepatic metabolism (29,30). The *in vivo* effectiveness of a two-pronged treatment strategy that i) directly targets tumor cells by way of combined BZ administration, and ii) indirectly suppresses tumor development and metastasis through gut-supporting/immune enhancing CMPs, was examined. In these studies, human breast cancer cell line, MDA-MB-468, (a cell line that is triple negative similar to the 4T1 cells used in our *in vivo* studies), was also included to determine the *in vitro* effectiveness of the BZs for possible use in the clinic. The advantage of co-administering OFZ/PBZ as opposed to monotherapies with single OFZ or PBZ was assessed in 3D spheroids using an aggressive human breast cancer cell line, MDA-MB-468 (39).

Materials and methods

Mice and in vivo studies. A total of 50 female BALB/c mice (8-10 weeks-old, weighing 18-22 g; Taconic Laboratories) were caged and used according to the National Institutes of Health guidelines, under protocols approved by Florida Atlantic University Institutional Animal Care and Use Committee (approval no. A21-15; Boca Raton, USA). Animals were housed under 12/12-h light/dark cycle in a climate-controlled colony. Colony temperature was kept at 18-23˚C, and animals had free access to food and water, housed in ventilated cage racks with HEPA filters. 4T1Br4 mammary tumor cells, an aggressive variant of the syngeneic triple negative phenotype 4T1 model selected for accelerated metastasis to the brain, were obtained from Dr Norman Pouliot (Olivia Newton-John Cancer Research Institute, Heidelberg, Australia). These cells when compared with the parental 4T1 cells have an enhanced ability to migrate across a brain-derived endothelial monolayer and adhere to endothelial cells and thus characterized for brain selectivity of 4T1Br4 tumors (38). 4T1Br4 cells were maintained in RPMI-1640 (Gibco; Thermo Fisher Scientific Inc.) with 10% fetal calf serum (HyClone; Cytiva) as previously reported (40). A total $0.3x10^5$ 4T1Br4 mammary tumor cells suspended in saline in 0.1 ml were implanted unilaterally in mammary fat pad in mice by orthotopic injections. Treatments with BZs and/or CMPs were initiated ~3 weeks post tumor

implantation, i.e., after seeding into lymph nodes as described below.

Administration of BZs and CMPs. ~1 week after tumor implantation, mice were randomly grouped (10 mice/group) under the following 5 experimental conditions: i) No treatment (10% DMSO); ii) CMPs, 10 mg/kg suspended in saline; iii) OFZ, 5 mg/kg dissolved in 10% DMSO; iv) PBZ, 9 mg/kg dissolved in 10% DMSO; and v) Combination BZs (OFZ + PBZ) and CMPs dissolved in 10% DMSO. A combination of BZs (OFZ/PBZ) was used to prevent possible resistance to treatment that could occur as previously described in anthelmintic therapeutic effects (30,41). CMPs (1-10 μM, kindly provided by Dr Yoshimi Shibata, Florida Atlantic University, FL, USA) were prepared as previously described (42,43). OFZ (cat. no. 1483301) and PBZ (cat. no. 1498706) were obtained from Sigma Aldrich; Merck KGaA. All the drugs and controls were administered orally in 200 μl per volume per mouse. The doses of the compounds administered match the best doses reported in veterinary assessments for hepatic delay of OFZ metabolism by PBZ co-administration that optimize anthelmintic effects (29,30) and previously published effective antitumor doses of CMPs (37). Treatments were administered by oral gavage on alternate days for up to 12 weeks starting at 3 weeks after tumor implantation, a time point at which metastasis to the lymph nodes is commonly reported. The mice were assessed for tumor volume and outliers (i.e., no tumor takes, either very small or very large) in each of the groups were excluded at the onset of the treatment to minimize biases. Mice were weighed weekly and observed daily for health check including measuring tumor size with a caliper. A tumor burden scoring system was adopted from University of Texas at El Paso to monitor the tumor-bearing mice, following standard guidelines for the welfare of animals (44-46). Mice were either euthanized based on body condition scores during health checks or were expired due to disease progression. Euthanasia occurred by cervical dislocation. At both disease end points necropsies were performed on mice including assessment of angiogenesis. In addition, fecal samples were collected weekly from each animal. Animals that had the same experimental assignment were home caged together. Fecal boluses were pooled per cage. These studies were repeated in multiple cohorts that were pooled at the end of the study.

Immunohistochemistry (IHC)

Ki-67. To determine if single OFZ, PBZ or dual BZ administration combined with CMPs has an impact on tumor progression, 4T1Br4 BALB/c tumor bearers were assessed by weekly primary tumor caliper measurements and body condition scoring. Metastasis to lungs and brain were assessed by gross morphological evaluations of tissue at euthanasia or post-expiration due to disease progression. In both of these instances of disease end point, tissue pertaining to tumor, lungs and brain were collected for downstream analyses. Post-fixed (in 4% paraformaldehyde at 4˚C overnight) and 30% sucrose-immersed (for at least 10 days) tumor tissue were snap frozen with isopentane cooled to -40˚C. Cryostat sections (20 μm) were assessed for proliferation by Ki-67 IHC following the standard protocol (47) using a primary anti-mouse Ki-67 antibody (1:500; cat. no. sc-23900; Santa Cruz Biotechnology, Inc.) and donkey anti-mouse Alexa Fluor 488 as the secondary antibody (1:1,000; cat. no. A-21202; Thermo Fisher Scientific, Inc.). Sections were incubated with 10% donkey serum (cat. no. ab7475; Abcam) in PBS in room temperature for 1 h to block non-specific binding. Primary antibody (in PBS with 10% donkey serum) incubation occurred in 4˚C overnight. Secondary antibody incubation occurred for 2 h in room temperature. Confocal imaged Ki-67-positive cells were analyzed using the ZEISS ZEN 3.1 (blue edition) automatic image analysis software. Sampling areas were set as 50 mμ X50 mμ (X-Y) and 10 mμ (Z) steps for a total of 3-4 sampling areas per section for 10 sections. Images were analyzed using ImageJ software (v1.54; National Institutes of Health), a method adapted from Shihan *et al* (48).

Free fatty acid receptor 2 (FFAR2). Cryostat sections (20 μm) of tumor and lung tissue were assessed for FFAR2 expression by IHC using anti-rabbit FFAR2 primary antibody (1:100; cat. no. AFR-032; Alomone Labs) followed by staining with secondary donkey anti-rabbit 594 antibody (1:1,000; cat. no. A-21207; Thermo Fisher Scientific, Inc.). Sections were incubated with 10% donkey serum in PBS in room temperature for 1 h to block non-specific binding. Primary antibody (in PBS with 10% donkey serum) incubation occurred in 4˚C overnight. Secondary antibody incubation occurred for 2 h in room temperature. Confocal microcopy images were analyzed using the Scion Image software (v4.0; Scion Corporation) to determine signal intensity (2.5X above background, expressed as optical density). FFAR2 expression in the brain was not assessed. Instead, metabolites of gut microbiota in the form of SCFAs present in the brain were directly quantified to identify multiple mechanistic targets for gut-brain cross talk.

Gross morphological assessment of metastasis. A previous studies by the authors revealed significantly decreased metastasis to the lung in 4T1 mammary tumor-bearing mice when CMPs are administered previous to tumor cell implantation (34). In the present study, to determine the effects on end-stage metastatic disease, treatment interventions were initiated after metastasis had been established in the lungs. A sentinel mouse was euthanized at 21 days post-tumor inoculation to verify metastasis to the lungs prior to start of the treatments. At the disease end point, tissue from the brain, lungs and the gastrointestinal (GI) tract were harvested for histologic analyses from all groups of mice. Tissue were snap frozen with isopentane cooled to -40˚C and stored in -80˚C until sectioning. Lungs and brain tissue were evaluated for metastatic invasion using gross morphological assessment. Sections were collected at 20 μm thickness at a systematic sampling interval of 120 μm through the lungs and brain using a cryostat cooled to -18˚C, and were stained using H&E according to the manufacturer's instructions (cat. no. H-3502; Vector Laboratories Inc.). Sections were analyzed for metastasis on an Olympus BH-2 light microscope at 4X, 10X and 20X magnifications. The images were examined and scored by a board-certified pathologist, Dr Robinson, in a double-blind fashion in terms of percentage of tissue on a section invaded by large metastatic accumulation or solid tumor growth. Percentage measures were likely underrepresented since scoring was restricted to gross morphology and therefore

excluded accounts of sparse cancer cells. For brain metastasis percentage of mice with solid brain tumors at disease end point were assessed as a descriptive measure.

Short chain fatty acid (SCFA) content analyses. Fecal boluses were analyzed at two time points: i) 3 weeks post cancer cell inoculation and before the onset of treatment, constituting the disease baseline; and ii) at disease end point when animals exited the study following different treatment interventions or received no treatment. Brain cortical biopsies were collected at euthanasia or expiration of the animal at disease end point and snap frozen in isopentane cooled to -40˚C. SCFA content analyses were outsourced to the Duke University Proteomic and Metabolomic Services. Briefly, an ultra-high performance liquid chromatography (UHPLC-MS/MS) method (49-51) was utilized to analyze SCFAs, including acetic acid, propionic acid, i-Butyric acid, butyric acid, 2-Me-Butyric acid, isovaleric acid, valeric acid, 3-Me-Valeric acid, i-Caproic acid, caproic acid, heptanoic acid and octanoic acid. The method utilizes an Acquity UPLC coupled to a Xevo TQ-S triple quadruple mass spectrometry by Waters Corporation to perform quantitative multiplexed analysis of the 12 SCFAs in fecal and brain samples. Samples were transported according to the Core Facility's specifications of quantity and collection scheme. Fecal SCFA measures were standardized according to baseline levels.

3D tumor spheroid multi-parametric assessment using MDA-MB-468 human cell line. The multiparametric assay used measures of i) the induction of cell death by following cell number based on DNA content using a nuclear stain that labels all cells, ii) early apoptotic events by following those cells positive for caspase cleavage but negative for 7-amino actinomycin D (7AAD), and iii) late apoptotic/necrotic cells by those positive for 7AAD but not caspase cleavage. The human triple negative breast cancer cell line MDA-MB-468 used in the present assay exhibits an invasive phenotype *in vitro*, and tumorigenic *in vivo* (39) and was used to establish clinical relevancy and assess the effectiveness of the treatments tested. Furthermore, these cells closely resemble 4T1 mouse mammary tumor cells used for the *in vivo* studies. MDA-MB-468 cells were purchased from the American Type Culture Collection (cat. no. HTB-132) and maintained as previously reported (52). Matrigel was purchased from BD Biosciences. Dimethyl sulfoxide (DMSO) was purchased from Thermo Fisher Scientific, Inc. The protocol used follows the authors' previously described methods (52). In 3D assay, the incubation time was reduced to 24 h to capture more cells in early apoptosis showing caspase 3 cleavage (53-55). Briefly, 1,500 MDA-MB-468 cells/well were plated on a black, clear bottom, low adherence spheroid 384-well tissue culture plate (cat. no. 3830; Corning, Inc.) in 30 μl ice-cold complete media without phenol red containing 2.5% Matrigel (BD Biosciences). A sphere was allowed to form overnight. After confirming the formation of a spheroid, 30 μl of medium containing treatment at two times the final concentration was added into each of the wells. Treatments consisted of 10, 5, 2.5 or 1.25 μM OFZ, 5, 2.5, 1.25 or 0.625 μM PBZ or a combination 10/5, 5/2.5, 2.5/1.25 or 1.25/0.625 μM OFZ and PBZ. Controls included 10 μM ABT-737, 5 μg/ml 5-fluorouracil, 0.5 μg/ml doxorubicin, media alone, and solvent controls. These controls are known to induce apoptosis at the concentrations used (52). These controls were used rather than taxanes since the objective of the assay was to measure induction of cell death, and taxanes sometimes induce cell cycle arrest rather than cell death depending on the concentration used (53,56-58). Solvent for drug treatments was 10% DMSO. Cells were incubated with treatment for 24 h at 37˚C CO_2 incubator after which 20 μl/well of a staining mixture containing 2 drops/ml NucBlue Live Cell Stain Hoechst 33342 (Molecular Probes; Thermo Fisher Scientific, Inc.), 5 μM CellEvent™ Caspase-3/7 Green Detection Reagent (Molecular Probes; Thermo Fisher Scientific, Inc.) and 100 μg 7AAD (MilliporeSigma) were added and allowed to incubate at 37˚C for an additional 3 h. Cells were then fixed with 4% paraformaldehyde for 30 min. Images were obtained using the ImageXpress® Micro XLS widefield HCS (Molecular Devices, LLC), with a 10X Plan Fluor objective, binning at 2 and focusing on plate bottom, then offset by bottom thickness. A stack of 8 images separated by 10 μm were acquired by starting at the well bottom and covering approximately the lower half of each spheroid. Multi-Wavelength Cell Scoring Module of the MetaXpress 5.1.0.3 software (Molecular Devices, LLC) was used to analyze the best focus projection of the stack acquired. The results were plotted using Microsoft excel (Office 365, v16.0; Microsoft Corporation). To normalize results, the solvent control values were subtracted from the 7AAD and the Caspase 3 percentage of positive results for treatment samples. Total cell count was expressed as a percentage comparing treatments with respective solvent controls. Compounds were tested in duplicate within plates.

2D cell viability assay (MTT) using MDA-MB-468 human cell line. To assess cell viability, the traditional MTT assay using cells plated in 2D at 72 h was used according to our previously published methods (52). Briefly, 3,000 cells per well in a volume of 30 μl/well were plated on a clear flat bottomed 384-well tissue culture plate and allowed to adhere for 24 h. After the incubation period, 30 μl of medium containing treatment at two times the final concentration was added. Treatments consisted of 10, 5, 2.5 or 1.25 μM OFZ, 5, 2.5, 1.25 or 0.625 μM PBZ or a combination 10/5, 5/2.5, 2.5/1.25 or 1.25/0.625 μM OFZ and PBZ. Controls included 5 μg/ml 5-fluorouracil, 0.5 μg/ml doxorubicin, media alone, and solvent controls. Solvent for drug treatments was 10% DMSO. The cells were then incubated for 72 h at 37˚C and 5% CO_2 after which 125 μg MTT was added to each well and incubated for 3 h at 37˚C. This was followed by centrifugation (314 x g for 10 min at 4˚C), the supernatant was then removed and 100 μl acidified isopropyl alcohol (1:500 solution of hydrochloric acid to isopropanol) was added to each well to dissolve the crystals. The absorbances of these solutions were measured at 570 nm with a plate reader (NOVOstar; BMG Labtech GmbH). The resulting absorbances were normalized against ethanol treated cells using Microsoft Excel.

Statistical analysis. Statview (v5.0; SAS Institute Inc.) was used for all statistical analyses. All data pertaining to *in vivo* percent survival, number of Ki-67 labeled cells in primary tumor, amounts of SCFAs in fecal and brain biopsy samples, FFAR2 signal in optical density in lungs and primary tumor

and percent metastatic invasion of lungs were analyzed by one-way ANOVAs using Groups as between subjects' variable (no treatment, CMPs, OFZ, PBZ and Combination of OFZ + PBZ + CMPs). Significant effects were followed with post-hoc comparisons using the Fisher's Least Significant Difference (LSD) test. Total cell counts expressed as percentage and cytotoxicity measures in MDA-MB-468 human breast cancer cells were analyzed using the unpaired Student's t-tests. Experiments were repeated a minimum of three times. Simple regression analyses were conducted between the FFAR2 optical density measures in primary tumor or lungs with the percent metastatic invasion of the lungs. $P<0.05$ was considered to indicate a statistically significant difference for all comparisons and main effects.

Results

Co-administration of BZs and CMPs enhances survival and decreases tumor cell proliferation. In the present study, the treatment effects on survival rates in mice bearing advanced 4T1Br4 mammary tumors were determined, i.e., treatment of mice starting at 3 weeks post-tumor implantation with BZs administered either singly or in combination with CMPs. Thus, mice in each of the groups received either single BZ (i.e., OFZ or PBZ) or CMP treatment or combination with OFZ + PBZ and CMPs on alternate days up to 12 weeks post tumor cell implantation (i.e., 12 weeks post-cancer cell inoculation is when all mice were either euthanized due to body condition score cut off or expired due to disease progression). Group sizes were as follows: i) no treatment (n=8), ii) OFZ (n=7), iii) PBZ (n=7), iv) CMP (n=7) and v) combination of BZs and CMPs (n=8). Percentages of mice surviving in groups were plotted across weeks (Fig. 1A). One-way ANOVAs revealed significant group differences at weeks 4-12 [$Fs_{(4,32)}>5.910$, $ps<0.0016$]. More importantly, post-hoc comparisons demonstrated that even though the treatments were started after establishment of metastasis to the lungs using the aggressive 4T1Br4 model, a 20% longer survival was observed in mice treated with a combination of OFZ, PBZ and CMPs compared with single drug treatments or no treatment groups at weeks 4-12 [$ps<0.002$]. There were no differences in the rate of survival in mice treated with OFZ alone or PBZ alone when these groups were compared with no treatment group. Contrary to the authors' previous studies using the 4T1 mammary tumor model showing enhanced survival in 4T1 mammary tumor-bearing mice when treated with CMPs prior to establishment of metastasis (34), survival was not enhanced in the aggressive 4T1 Br4 tumor bearers treated with CMPs alone compared with no treatment controls (Fig. 1A). The most significant observation was that mice treated singly with either CMPs, OFZ, or PBZ did not survive past 6 weeks while some of the mice in combination group survived ~6 weeks longer than the groups that received monotherapy. These results may be ascribed to the effect of BZs on microtubules combined with the effect of CMPs on the immune system and the gut. Untreated mice were more prone to be euthanized due to reaching body condition score cut off at health checks at an earlier time point due to extensive metastasis than mice belonging to any other groups (data not shown).

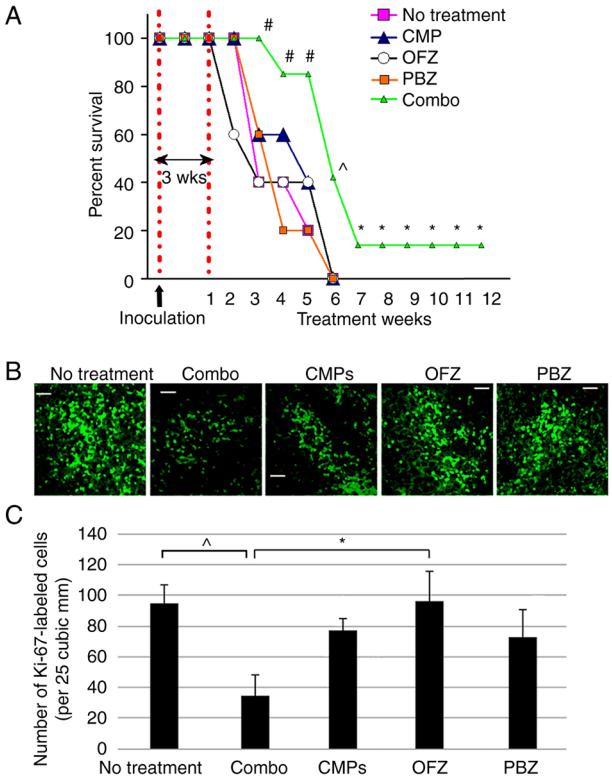

Figure 1. Combination treatment with BZs (OFZ + PBZ) and CMPs increase survival and decrease tumor cell proliferation in 4T1Br4 mammary tumor-bearing mice. (A) Comparisons between dual BZs with CMPs vs. single treatment with OFZ, PBZ, CMPs or no treatment. (B) Expression of Ki-67 (green immunofluorescence) in tumor tissue was analyzed by confocal microscopy. Scale bars, 20 μm. (C) Decreased number of cells labeled with Ki-67 in combination (OFZ/PBZ and CMP)-treated compared with untreated, or those treated with OFZ alone. Bar graphs represent the mean + SEM. $^{*}P<0.05$, $^{\wedge}P<0.01$ and $^{\#}P<0.001$. BZs, benzimidazoles; OFZ, oxfendazole; PBZ, parbendazole; CMPs, chitin microparticles.

Since BZs are known microtubule inhibitors, tumor cell proliferation was determined by the Ki-67 assay across treatment groups (Fig. 1B). One-way ANOVA showed significant group differences in number of Ki-67-labeled cells in tumor tissue [$Fs_{(4,32)}=2.723$, $P=0.046$; Fig. 1C]. Post-hoc comparisons identified lower number of Ki-67-labeled tumor cells in combination BZs compared with single OFZ treated mice ($P=0.044$) or no treatment group ($P=0.002$). Mice that received no treatment and those that received single OFZ treatment had comparable numbers of Ki-67-labeled cells. These data indicated that BZs in combination with CMP prolonged the survival and reduced the tumor burden by inhibiting tumor cell proliferation.

SCFA levels in the gut and the brain following co-administration of BZs and CMPs. Bidirectional interactions between the host and the microbiome occur via secretion of bacterial metabolites that include SCFAs that could then have an effect on tumor progression. Therefore, the levels of SCFAs in the gut and the brain were assessed as this tumor model is known to rapidly metastasize to the brain. One-way ANOVAs were used to analyze 12 SCFA amounts in the fecal (adjusted to baseline levels) and brain biopsy samples from five groups of animals [no treatment controls (n=7), single OFZ (n=6) or

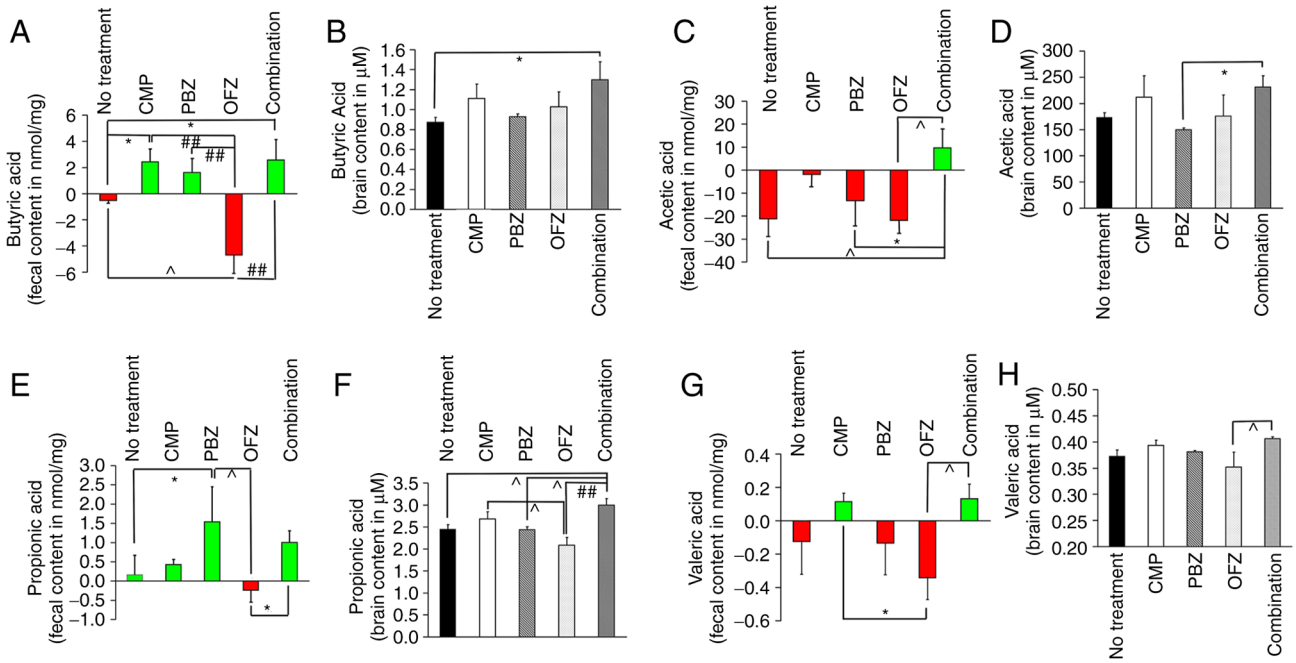

Figure 2. Ultra-high-performance liquid chromatography analysis of short-chain fatty acid content in fecal and brain samples. (A and B) Butyric acid, (C and D) acetic acid, (E and F) propionic acid and (G and H) valeric acid data are plotted for (A, C, E, G) fecal and (B, D, F, H) brain samples. *P<0.05, ^P<0.01 and ##P<0.0001. CMPs, chitin microparticles; OFZ, oxfendazole; PBZ, parbendazole.

PBZ (n=6) treated animals, single CMP (n=6) treated animals and combination BZ and CMP (n=7) treated animals; Fig. 2]. Significant effects were detected in fecal butyric (Fig. 2A), acetic (Fig. 2C), propionic (Fig. 2E) and valeric acid (Fig. 2G) levels between groups [$Fs_{(4,27)}$>2.202, ps<0.044]. Specifically, combination of BZs and CMPs led to increased fecal butyric and acetic acid levels compared with no treatment controls (ps<0.013). Combination of BZs and CMPs also led to increased fecal butyric and acetic acid levels compared with single OFZ or PBZ administrations (ps<0.036). Single CMP treated mice also showed increased fecal butyric acid levels compared with no treatment controls (P=0.022). There was a significant decrease in fecal butyric acid levels in OFZ-treated mice compared with PBZ-treated or no treatment control mice [ps<0.002]. Moreover, OFZ monotherapy led to a significant reduction in fecal propionic and valeric acid contents in comparison with levels observed in single PBZ or combination BZ and CMP treated mice for propionic acid [ps<0.033], and single CMP or combination BZ and CMP treated mice for valeric acid [ps<0.015]. Interestingly, monotherapy with PBZ caused an increase in fecal propionic acid levels compared with levels observed in no treatment controls (P=0.012), which is a contrast to the reduction identified following OFZ monotherapy. Furthermore, significant effects were detected in butyric (Fig. 2B), and propionic acid (Fig. 2F) levels in brain biopsy samples between groups [$Fs_{(4,27)}$>2.238, ps<0.091]. In parallel with the fecal samples, brain biopsy samples also demonstrated an increase in levels of butyric acid in combination of BZ and CMP-treated mice compared with no treatment controls (P=0.013). Brain biopsy samples depicted wide range of effects in propionic acid levels, namely combination of BZ and CMP-treated animals demonstrating an increase compared with no treatment or PBZ monotherapy groups (ps<0.002). CMP single treatment resulted in higher levels of propionic acid in brain biopsy samples compared with OFZ single treatment (P=0.002). Lastly, combination BZ and CMP treatment resulted in higher levels of acetic acid and valeric acid in brain biopsy samples compared with PBZ (P=0.033) and OFZ (P=0.005) monotherapies respectively (Fig. 2D and H). H&E histochemistry was used to assess the morphology of the GI tract to determine if BZs and CMPs have an effect on the structural integrity of the GI tract. None of the groups demonstrated necrosis or inflammation of the mucosa. The bowel mucosa was viable in the GI tracts of all the groups indicating no differences between the untreated versus combination BZ and CMP treatment or individual monotherapy conditions (data not shown).

FFAR2 expression in tumor and lungs following single BZ, CMP or combination BZ and CMP treatments. As SCFAs are known to mediate their effects through G-protein-coupled receptors such as FFAR2 (59), the expression of FFAR2 in the primary tumor tissue and in the lungs was evaluated. The first tissue was for breast cancer metastasis between groups [no treatment (n=8), OFZ (n=7), PBZ (n=7), CMP (n=7), Combination of BZs and CMP (n=8)]. The FFAR2 labeling was quantified as optical density (signal, Fig. 3) and analyzed in the tumor and lungs by one-way ANOVAs. A significant group difference was detected in FFAR2 levels in the primary tumor at the disease end point ($Fs_{(4,32)}$=3.904; P=0.010). Specifically, higher expression of FFAR2 was detected in the tumor tissue of mice receiving combination of BZ and CMP treatment compared with no treatment control mice (P=0.006; Fig. 3A and B). The combination BZs and CMPs also resulted in higher FFAR2 levels in primary tumor compared with PBZ monotherapy group (P=0.001; Fig. 3A and B). In contrast to the tumor tissue, the groups treated with CMPs had the highest levels of FFAR2 expression in the lungs ($Fs_{(4,32)}$=3.713, P=0.013; Fig. 3C and D)

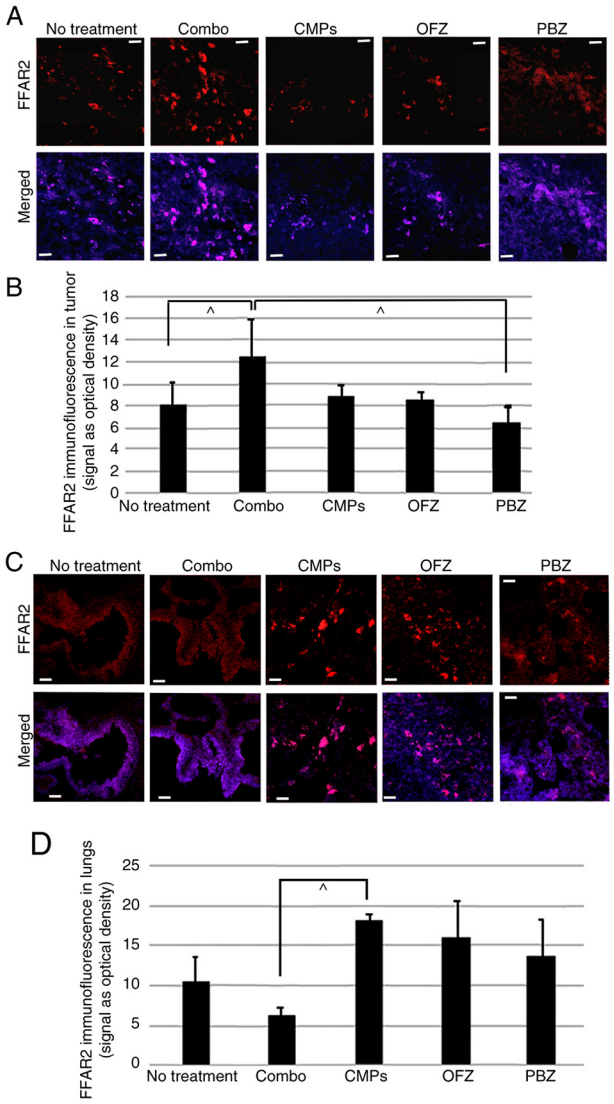

Figure 3. Expression of FFAR2 in tumor and lung tissue assessed by immunofluorescence microscopy. X-Y-Z sampling was converted to maximum intensity projection images and analyzed by Scion Image software for optical density of gray scale transformed images. Data are presented as optical density with signal defined as at least 2.5X the background. Red fluorescence represents FFAR2 expression in tissue, and blue represents DAPI labeling. FFAR2 expression in (A and B) tumor and (C and D) lung tissue in the combination BZs (OFZ + PBZ) and CMP treatment group compared with those from untreated and single BZ treated mice. Bar graphs represent the mean + SEM. ^P<0.01. FFAR2, free fatty acid receptor 2; BZs, benzimidazoles; OFZ, oxfendazole; PBZ, parbendazole; CMPs, chitin microparticles.

and this effect was significant in levels from mice treated with CMP monotherapy compared with mice treated with combination of BZs and CMPs (P=0.006). Mice treated with OFZ and to some extent PBZ also expressed FFAR2 in the lungs but the levels were less than those in the CMP-treated mice.

Decreased metastasis to the lungs and brain in mice receiving co-administration of BZs and CMPs. Gross morphological assessments of lungs and brain tissue from mice treated with single OFZ, PBZ, CMPs or combination of BZs and CMPs were compared with tissue analyzed from untreated control mice at metastatic breast cancer disease end point (Fig. 4). Histologic images of lungs from untreated mice revealed widespread narrowing of alveoli and/or solid mass of carcinoma cells (Fig. 4A) while lung tissue from tumor-bearing mice treated with OFZ (Fig. 4B), PBZ (Fig. 4C) and CMPs (Fig. 4D) demonstrated partially normal appearing lung tissue with respiratory bronchioles and alveolar ducts with no carcinoma cells present intercepted with accumulation of cancer cells. In each of the mono treated CMPs, OFZ or PBZ representative image, carcinoma is present (Fig. 4B-D). By contrast, combination of BZ and CMP-treated mice showed <20% of the lung tissue showing signs of metastasis at disease end point, and images were largely clear of carcinoma (Fig. 4E and F). A one-way ANOVA with groups [untreated (n=8), combination pf BZs and CMPs (n=8), single CMPs (n=7), single OFZ (n=7), and single PBZ (n=7)] as between subjects variable revealed a significant group effect [$F_{(4,32)}$=15.50, P<0.0001; Fig. 4F]. Post-hoc comparisons showed significant differences between untreated versus combination-treated, untreated versus single CMP-treated; untreated versus single OFZ-treated and untreated versus single PBZ-treated groups in the direction of higher percentage of lung metastasis in untreated mice compared with various treatment groups [ps<0.001]. The largest effect was detected between untreated and combination treatment groups with ~4X higher percentage of metastasis observed in the untreated group in comparison with mice that received combination treatment. Combination versus single CMP (P=0.023) and combination versus single OFZ [P=0.0028] comparisons also demonstrated effects in the direction of significantly less percentage of metastasis in combination group compared with CMP and OFZ monotherapy. Tissue sections of the brain were stained by H&E to determine metastasis. No visible metastases were observed in brain sections from combination of BZ and CMP-treated mice, which showed a stark contrast of >80% of mice from untreated group exhibiting brain tumor mass at disease end point (Fig. 4G-I), suggesting that brain metastasis is common at disease end point in this animal model.

FFAR2 in the primary tumor is negatively associated with lung metastasis. Simple regression analyses were conducted between levels of FFAR2 in lungs and primary tumor (Fig. 3) with percent lung metastasis (Fig. 4F). Values were pooled for all experimental and control mice [untreated (n=8), OFZ (n=7), PBZ (n=7), CMP (n=7), Combination BZs and CMP (n=8)]. No association was detected between FFAR2 IHC in lungs with percent lung metastasis [$F_{(1,36)}$=0.221, P=0.641, data not shown]. However a negative association was found between the FFAR2 expression in the primary tumor and the percent lung metastasis [$F_{(1,36)}$=9.173, P=0.004; Fig. 4G].

Effects of OFZ and PBZ as monotherapy or co-administered as combination BZs on human breast cancer cell (MDA-MB-468) spheroids. To determine the effectiveness and clinical relevancy of co-administration of OFZ and PBZ in comparison with BZ monotherapies, MDA-MB-468 spheroids were incubated in the presence of OFZ and PBZ singly or in combination at different doses as aforementioned for 24 h. Three independent experiments were performed. The images from one representative experiment are depicted in Fig. 5A. Images were analyzed to determine cell counts based on nuclear staining (Hoechst 33342 stain; blue; Fig. 5A),

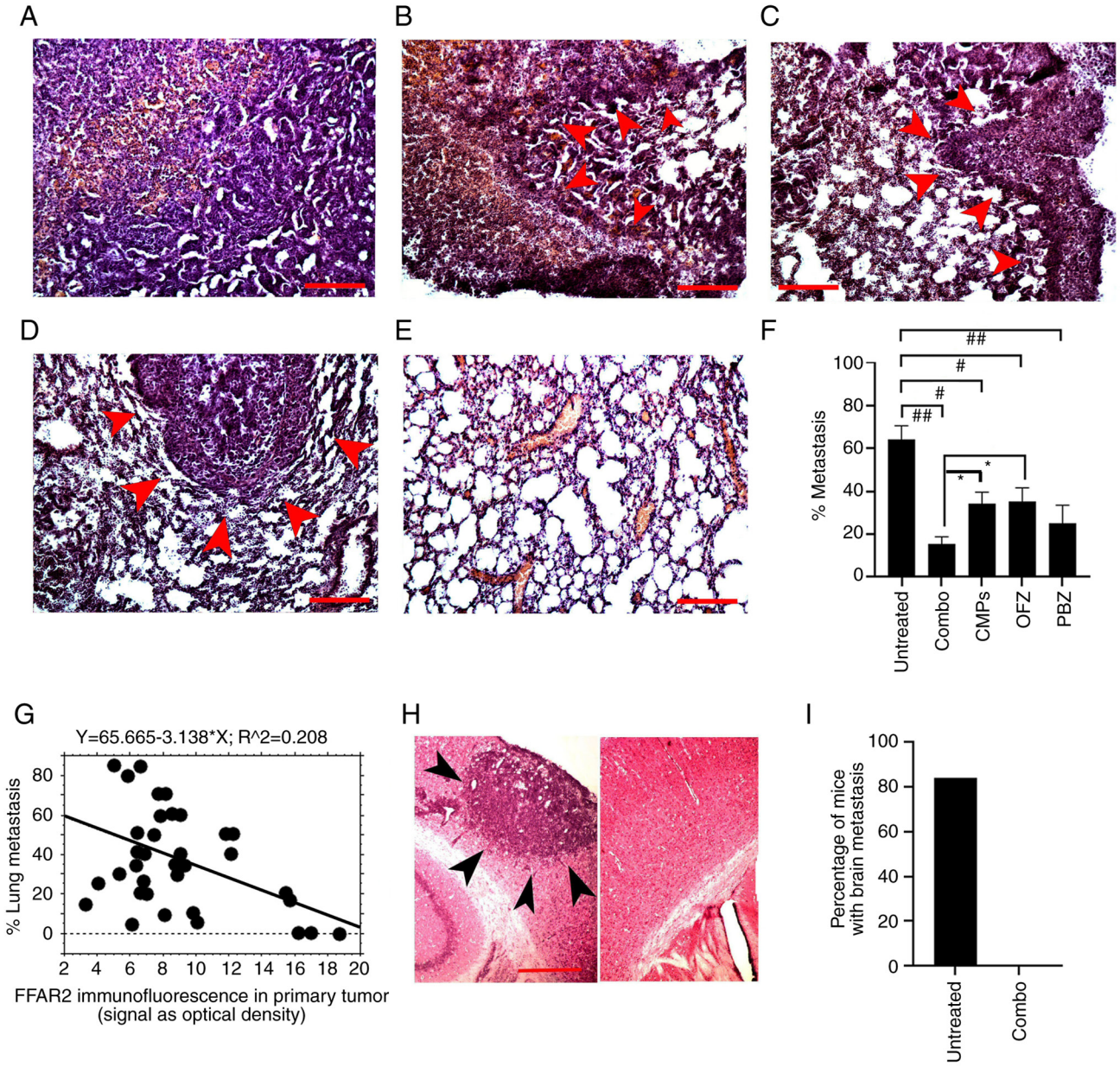

Figure 4. Metastatic invasion to the lungs and brain. Representative H&E sections from the lungs: (A) No treatment showing constriction of bronchioles and/or solid mass carcinoma, (B) single OFZ or (C) PBZ or (D) CMP treatment and (E) combination BZs and CMP treatment showing largely normal lung tissue with respiratory bronchioles and alveolar ducts. Moreover, representative sections from mice treated with single BZs [OFZ, (B); PBZ, (C)] and single CMPs (D) all showed some normal alveolar tissue with alveolar ducts visible simultaneously with invasion of tumor cells (red arrows pointing at metastatic mass). (F) The percentage of the tissue demonstrating visible metastatic invasion in gross morphology was quantified at each sampled section (15-20 sections per animal per tissue) by a pathologist. (G) Simple regression scatter plot depicting a negative association between the extent of lung metastasis and the levels of the fatty acid receptor 2 (FFAR2) in the primary tumor. Representative H&E sections from the brain are shown for tumor-bearing no treatment (panel H, Left) and tumor non-bearing combination treatment (panel H, Right). (I) Number of mice depicting brain tumors at disease end point was plotted as group percentages for combination BZ and CMP treated mice compared with percentage seen in no treatment controls. Black arrows in panel H indicate the brain tumor mass from a representative no treatment mouse. Scale bars, 250 μm. Bar graphs represent the mean + SEM. *P<0.05, $^{\#}$P<0.001 and $^{\#\#}$P<0.0001. OFZ, oxfendazole; PBZ, parbendazole; CMPs, chitin microparticles; BZs, benzimidazoles.

percentages of cells dying through apoptosis by following cleavage of caspase 3 (green; Fig. 5A), and percentages of cells dead or dying through late apoptosis/necrosis as measured by the loss of their membrane integrity (7AAD; red, Fig. 5A). These results revealed that both OFZ and PBZ demonstrated activity in a dose-dependent manner in all measures assessed (Fig. 5B). In general, PBZ was statistically more potent at all concentrations tested than OFZ, indicated by higher activity at even lowest doses in all measures plotted. Moreover, OFZ resulted in primarily loss of cell membrane integrity (i.e., 7AAD counts), while PBZ resulted in primarily caspase cleavage suggesting induction of apoptosis [ps<0.05]. In this cell line, the co-administration of OFZ and PBZ performed better than the individual drugs as there were significant increases in the number of dead or dying cells based on 7AAD at all concentrations [Fig. 5B; ps<0.02]. In addition, there was a significant increase in the number of cells showing caspase cleavage at the lower OFZ/PBZ combination doses compared

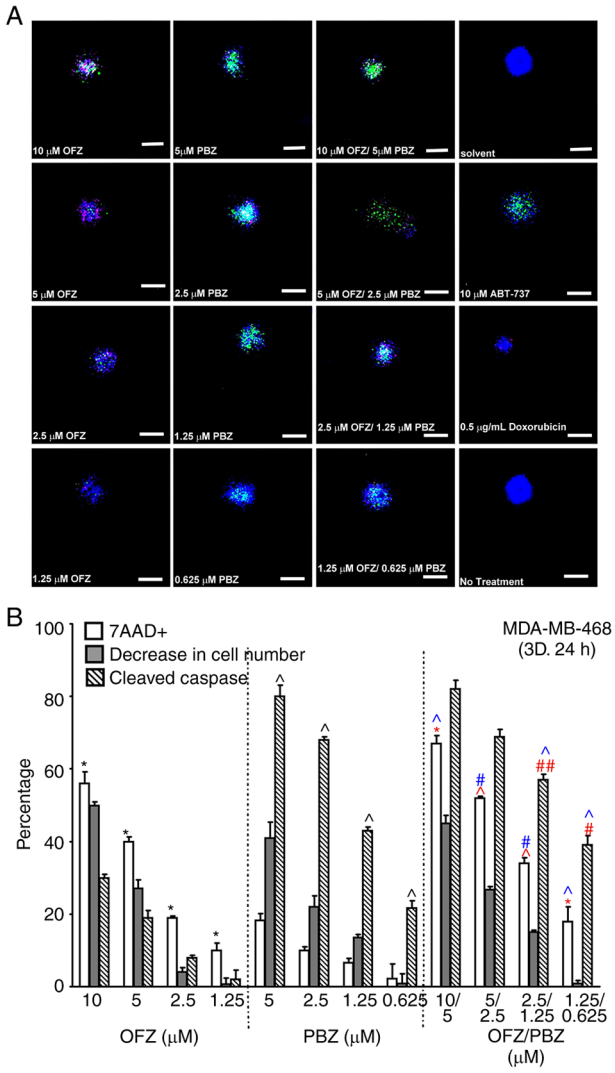

Figure 5. MDA-MB-468 spheroid multiparametric assessment of viability after treatment with OFZ (10, 5, 2.5, or 1.25 μM concentrations) PBZ (1.25 or 0.625 μM concentrations) or a combination of OFZ and PBZ (BZs) (10/5, 5/2.5, 2.5/1.25 or 1.25/0.625 μM concentrations). Media alone was used as a negative control. ABT737 (10 μM), 5-fluorouracil (5 μg/ml) and doxorubicin (0.5 μg/ml) were used as positive controls. The overall control for the treatments was the solvent control. After the 24-h treatments, cells were labeled for 3 h with a reagent that fluoresces green when caspase 3/7 is cleaved and suggests apoptosis is occurring, and the nuclear stains Hoechst 33342 (blue), a permeable stain that labels all cells, and 7AAD (red), an impermeable stain that labels all dead, late apoptotic or necrotic cells that have lost membrane integrity. Cells were fixed and images acquired using a high content imager at 10X magnification. Scale bars, 200 μm. (A) Images from one representative experiment are shown. (B) The results from the analyses of the images from the 3D assay for the three independent experiments were averaged and bar graphed. The solvent control values for 7AAD and the Caspase 3 were subtracted from the treated values to normalize the data. Red significance markers are values of OFZ/PBZ compared with OFZ monotherapy of identical concentration; Blue significance markers are values of OFZ/PBZ compared with PBZ monotherapy of identical concentration. Significant comparisons between single OFZ and single PBZ treatments are indicated by black significance markers. Bar graphs represent the mean + SEM. *P<0.05, $^{\wedge}$P<0.01, $^{\#}$P<0.001 and $^{\#\#}$P<0.0001. OFZ, oxfendazole; PBZ, parbendazole; BZs, benzimidazoles.

with same doses applied in monotherapies [OFZ/PBZ: 2.5/1.25 and 1.25/0.625 μM; ps<0.05]. In addition to testing in spheroids, cells were also tested with the same combinations in the traditional 2D assay for 72 h. In this format, the activity of OFZ and PBZ were largely similar and there was not a distinct dose-dependency in single BZ or combination therapies. (data not shown). In addition, the combination of the drugs did not differ from single treatments of OFZ and PBZ (data not shown). CMPs were not included in the *in vitro* studies for the following reasons: i) CMPs function mainly through activating the immune system or, ii) via control of the gut microbiome, and iii) are not known to have a direct effect on tumor cells.

Discussion

The present study, to the best of the authors' knowledge, was the first to identify that increased survival can be achieved for late-stage cancers with combination therapy using BZs and CMPs. In contrast to conventional chemotherapeutics, taxanes and vinca alkaloids, BZs are well tolerated with low toxicity index, easily accessible and affordable, and have been in use in the field of anti-parasitic treatment for decades (14,60,61). Hence BZs constitute candidate drugs for rapid repurposing for primary and/or adjuvant cancer treatment. Dose-dependent toxicity and acquired resistance are both common problems with vinca alkaloids and taxanes used in chemotherapy (62,63). A caveat in transitioning BZs from acute parasitic application to a long-term, sustained cancer treatment is extending the therapeutic time window without resistance building to cytotoxic effects of the drug (61,64). For this reason, a special combination of BZs that consists of OFZ and PBZ co-administration orally, was employed. PBZ co-administration results in transient delay in OFZ metabolism (29,30) thereby increasing the length of therapeutic time window for microtubule binding effects. In addition, multiple bioactive BZs, namely OFZ, FBZ and FBZ sulphone (FBZ-SO_2) are reported detectable in plasma due to slow clearance of OFZ (29,30) potentially amplifying antitumor effects of parent drugs. Thus, using a novel combinatory approach with oral co-administration of multiple BZs (OFZ + PBZ) together with CMPs, a ~20% increase in survival of mice bearing an aggressive triple negative 4T1 Br4 breast-cancer that rapidly metastasizes to the brain (38), was previously reported by the authors. Even though the treatments were started late in disease progression, i.e., after metastasis had been established, the combination of BZs with CMPs administered orally prolonged the survival with decreased metastasis to the lungs and the brain, providing proof of concept evidence for therapeutic potential. Monotherapy with OFZ, PBZ or CMPs did not produce a significant effect in survival at this late stage compared with untreated control mice, although they did lead to lower percentages of metastasis in the lungs.

The present data indicated that increased survival with co-administration of OFZ/PBZ and CMPs is associated with decreased metastasis to the lungs and brain compared with untreated mice. It was revealed that there was <20% metastasis in the combination-treated group while there was >60% metastasis in the untreated group. The decreased metastasis to the lungs could partly explain the increased survival in the combination treated group. The data of the present study also demonstrated that >80% of untreated mice developed solid brain tumors detectable by gross morphological analyses at the disease end point, confirming that the 4T1Br4 model

does indeed rapidly progress to brain metastasis (38). In comparison none of the mice in combination-treatment group developed solid brain tumors. The risk of brain metastasis is usually highest for women who have triple negative breast cancer (65,66). It is unclear whether the lack of formation of solid brain mass in combination-treated mice reflects the treatment effectiveness or delayed metastasis to the brain since combination-treated mice might be meeting body condition criteria to be euthanized before brain metastasis occurs. Present findings do not rule out possibility of micro metastasis to the brain since only solid tumors were counted in this assessment. Even with the possibility of micro metastasis, the finding of complete lack of solid cancer mass in the brains of mice receiving combination treatment at a late stage is of significance.

In addition to increased survival and decreased metastasis, it was identified that the combination BZ and CMP treatment led to decreased proliferative index (i.e., Ki-67 expression) in the primary tumor compared with untreated mice, and no other treatment group tested was effective in suppressing proliferation in post metastatic stage of the cancer. Even though BZs are known for inhibiting microtubule formation along with decreased cell proliferation, treatment with BZs singly did not significantly affect proliferation rates. It is possible that the effects observed in the present study are due to variation in affinity for mammalian tubulin (67). Dogra *et al* (67) reported that FBZ exhibits moderated microtubule depolymerizing activity but has a potent antitumor effect. It is possible that the effects observed in the present study are due to synergistic effects of CMPs and BZs. A previous study by the authors showed decreased growth and metastasis in 4T1 mammary tumor-bearers treated with CMPs prior to tumor development and tumor reduction was ascribed to IFN-γ production and a shift in T cells from TH2 to TH1 (34). In the present study however, treatment of 4T1Br4 mammary tumor-bearers with CMPs alone did not decrease tumor cell proliferation. This is likely because treatments in the current study were started when mice already had a large tumor burden with metastasis to the lungs and thus the immune system could have been overwhelmed at this advanced stage.

It is known that dysbiosis with altered microbiome and decreased SCFAs can promote tumor progression while commensal bacterial-produced SCFAs have tumor-suppressing effects (68,69). Thus, the effect of BZs and CMPs treatment on the gut-derived compounds was assessed in the present study. Previous findings of decreased metastasis in 4T1 tumor-bearers treated with CMPs could have been due to the effects of CMPs on immune system (34) as well as its effects on the gut as chitin and its derivatives were revealed to influence gut microbiota (70) and modulate microbial environment in the colons of inflammation-induced mice (71). BZs and CMPs therapeutic treatments were therefore evaluated on the gut microbiome-derived SCFA content in fecal and brain biopsy samples as SCFAs traverse to other organs that are candidates for metastasis following their production in the gut. It was observed that butyric, acetic, propionic and valeric acid levels were increased in fecal samples following combination of OFZ/PBZ and CMP treatment. SCFAs such as butyrate, acetate and propionate are anti-inflammatory and act as 'gut calming' agents in the local digestive environment (72) and may induce antitumorigenic function in brain microenvironment. Increases in brain biopsies were simultaneously confirmed for levels of the butyric and propionic acid in combination of OFZ/PBZ and CMP-treated group compared with untreated mice. Fecal levels of butyric, propionic and valeric acids were also increased with CMP monotherapy. Similarly, fecal levels of butyric and propionic acid were found increased with PBZ monotherapy. However, none of these effects carried onto brain biopsy samples as compared with levels observed in untreated mice. Additionally, primary tumors from the OFZ/PBZ and CMP-treated mice exhibited increased levels of the FFAR2 which is a G-protein coupled receptor for SCFAs with inhibitory properties for cancer cell invasiveness and metastatic potential (13). The signaling molecules between gut and brain that regulate microglial homeostasis were identified to be SCFAs as mice deficient for SCFA receptor FFAR2 displayed maturational defects found in germ-free mice (41). In fact, Liu *et al* (73) reported that alveolar macrophages and alveolar type II cells express FFAR2 and that SCFAs can influence lung physiology. In line with this, a strong negative association between FFAR2 levels in primary tumor and levels of cancer metastasis to the lungs was revealed in the present study. It is also possible that CMPs activate lung macrophages to further increase FFAR2 expression in the pulmonary microenvironment, but this may not occur in the tumor microenvironment due to composition of the immune cells at this site. It may be hypothesized that SCFAs produced in the gut likely influence the lungs and drive FFAR2 expression to reduce metastasis to the lungs and then onto the brain. The present study highlighted the importance of combination therapy that uses BZs which have a direct inhibitory effect on tumor cells and CMPs that affect the gut and immune system for late-stage breast cancer patients whose tumors have metastasized to distant sites. Furthermore, SCFAs can readily cross the blood-brain barrier and affect the central nervous system directly (74). Similarly, BZs can also cross the blood-brain barrier as they have been found to treat parasitic infections of the nervous system and utilized in some rodent models of brain tumors (15,16,31). However, signaling mechanisms get more complex when downstream pathways are considered and future studies are needed such as identification of specific effects of SCFAs in microglial function in breast to brain metastasis in the 4T1Br4 tumor model.

The effects of BZs were further tested in 3D spheroids using MDA-MB-468, a cell line similar to the mouse 4T1Br4 cell line used in the current *in vivo* studies. OFZ and PBZ treatments alone demonstrated a dose response, with PBZ being more potent; OFZ showed more loss of membrane integrity while PBZ treatment led to more caspase cleavage. OFZ and PBZ combination treatment resulted in higher cell death compared with OFZ alone and in some cases to PBZ alone. The lowest concentrations of OFZ and PBZ co-administered resulted in an increase in caspase cleavage providing support for potential clinical effectiveness. Very different responses resulted when testing potential drugs against cells grown as spheroids (3D) compared with single layers (2D), with the 3D model having enhanced predictability of clinical effectiveness (75-77). Compared with 2D assays, spheroids (3D cell culture) have more cell-to-cell interactions, more interactions with the extracellular matrix and nutrient and oxygen

gradients; thus, they more clearly resemble tumor growth. These observations are consistent with other studies using BZ derivatives on glioblastoma 3D tumor spheroids in reducing tumor cell populations and reduction in spheroid size (78).

In summary, effectiveness of dual BZs combined with CMPs for late-stage breast cancer was demonstrated. Although numerous *in vitro* studies reported that BZs exhibit microtubule inhibitory activity (79), induction of apoptosis, suppression of proliferation, inhibition of angiogenesis and metastasis (80-86), to the best of the authors' knowledge, there are no *in vivo* studies in literature using this specific combinatory application of BZs (OFZ/PBZ) for anticancer effects. It is very promising that these treatments did not adversely affect the host unlike other conventional chemotherapeutics in use. Similarly, to the best of the authors' knowledge, there is no other study testing gut-altering compounds such as CMPs for treatment of late-stage breast cancer. The present study is the starting point for future studies in determining the mechanisms of combination therapies involving interactions with the gut and the immune systems that have downstream effects on tumor progression/regression.

Acknowledgements

Not applicable.

Funding

The present study was supported by FAU Stiles-Nicholson Brain Institute (grant no. F0019EG). Testing on triple negative breast cancer cells in 2D and 3D was supported by the Florida Department of Health (grant no. 9BC01).

Availability of data and materials

The datasets used and/or analyzed during the current study are available from the corresponding author on reasonable request.

Authors' contributions

VI and CI conceptualized and supervised the study, conducted formal analysis, acquired funding, performed project administration, provided resources, visualized data, wrote the original draft, and wrote, reviewed and edited the manuscript. RS conducted data curation, formal analysis, and contributed to writing the manuscript. PR curated data and edited the manuscript. EG conducted data curation and formal analysis, and contributed to writing the manuscript. AT and JLP conducted data curation and formal analysis. VI and CI confirm the authenticity of all the raw data. All authors read and approved the final manuscript.

Ethics approval and consent to participate

Animal experiments were conducted under an animal protocol approved (approval no. A21-15) by the FAU Institutional Animal Care and Use Committee (Boca Raton, USA). Animal experiments have been conducted according to National Institutes of Health guide for the care and use of laboratory animals. All animal studies complied with the ARRIVE guidelines and the AVMA euthanasia guidelines 2020.

Patient consent for publication

Not applicable.

Competing interests

Dr Iragavarapu and Dr Isgor have a patent pending for the combination treatment intervention included in this manuscript. The remaining authors declare that they have no competing interests.

References

1. Bou Zerdan M, Ghorayeb T, Saliba F, Allam S, Bou Zerdan M, Yaghi M, Bilani N, Jaafar R and Nahleh Z: Triple negative breast cancer: Updates on classification and treatment in 2021. Cancers (Basel) 14: 1253, 2022.
2. Li X, Yang J, Peng L, Sahin AA, Huo L, Ward KC, O'Regan R, Torres MA and Meisel JL: Triple-negative breast cancer has worse overall survival and cause-specific survival than non-triple-negative breast cancer. Breast Cancer Res Treat 161: 279-287, 2017.
3. Jhan JR and Andrechek ER: Triple-negative breast cancer and the potential for targeted therapy. Pharmacogenomics 18: 1595-1609, 2017.
4. Tutt ANJ, Garber JE and Geyer CE Jr: Adjuvant olaparib in BRCA-mutated breast cancer. Reply. N Engl J Med 385: 1440, 2021.
5. Yin J, Zhou C, Wang G and Gu J: Treatment for triple-negative breast cancer: An umbrella review of meta-analyses. Int J Gen Med 15: 5901-5914, 2022.
6. Zagami P and Carey LA: Triple negative breast cancer: Pitfalls and progress. NPJ Breast Cancer 8: 95, 2022.
7. Baranova A, Krasnoselskyi M, Starikov V, Kartashov S, Zhulkevych I, Vlasenko V, Oleshko K, Bilodid O, Sadchikova M and Vinnyk Y: Triple-negative breast cancer: Current treatment strategies and factors of negative prognosis. J Med Life 15: 153-161, 2022.
8. Pedersen RN, Esen BÖ, Mellemkjær L, Christiansen P, Ejlertsen B, Lash TL, Nørgaard M and Cronin-Fenton D: The incidence of breast cancer recurrence 10-32 years after primary diagnosis. J Natl Cancer Inst 114: 391-399, 2022.
9. Landry I, Sumbly V and Vest M: Advancements in the treatment of triple-negative breast cancer: A narrative review of the literature. Cureus 14: e21970, 2022.
10. Buchta Rosean C, Bostic RR, Ferey JCM, Feng TY, Azar FN, Tung KS, Dozmorov MG, Smirnova E, Bos PD and Rutkowski MR: Preexisting commensal dysbiosis is a host-intrinsic regulator of tissue inflammation and tumor cell dissemination in hormone receptor-positive breast cancer. Cancer Res 79: 3662-3675, 2019.
11. Kim CH: Control of lymphocyte functions by gut microbiota-derived short-chain fatty acids. Cell Mol Immunol 18: 1161-1171, 2021.
12. Rossi T, Vergara D, Fanini F, Maffia M, Bravaccini S and Pirini F: Microbiota-derived metabolites in tumor progression and metastasis. Int J Mol Sci 21: 5786, 2020.
13. Thirunavukkarasan M, Wang C, Rao A, Hind T, Teo YR, Siddiquee AA, Goghari MAI, Kumar AP and Herr DR: Short-chain fatty acid receptors inhibit invasive phenotypes in breast cancer cells. PLoS One 12: e0186334, 2017.
14. Son DS, Lee ES and Adunyah SE: The antitumor potentials of benzimidazole anthelmintics as repurposing drugs. Immune Netw 20: e29, 2020.
15. Bai RY, Staedtke V, Wanjiku T, Rudek MA, Joshi A, Gallia GL and Riggins GJ: Brain penetration and efficacy of different mebendazole polymorphs in a mouse brain tumor model. Clin Cancer Res 21: 3462-3470, 2015.
16. De Witt M, Gamble A, Hanson D, Markowitz D, Powell C, Al Dimassi S, Atlas M, Boockvar J, Ruggieri R and Symons M: Repurposing mebendazole as a replacement for vincristine for the treatment of brain tumors. Mol Med 23: 50-56, 2017.
17. Bai RY, Staedtke V, Aprhys CM, Gallia GL and Riggins GJ: Antiparasitic mebendazole shows survival benefit in 2 preclinical models of glioblastoma multiforme. Neuro Oncol 13: 974-982, 2011.
18. Zhang L, Bochkur Dratver M, Yazal T, Dong K, Nguyen A, Yu G, Dao A, Bochkur Dratver M, Duhachek-Muggy S, Bhat K, *et al*: Mebendazole potentiates radiation therapy in triple-negative breast cancer. Int J Radiat Oncol Biol Phys 103: 195-207, 2019.

19. Gao P, Dang CV and Watson J: Unexpected antitumorigenic effect of fenbendazole when combined with supplementary vitamins. J Am Assoc Lab Anim Sci 47: 37-40, 2008.
20. Choi HS, Ko YS, Jin H, Kang KM, Ha IB, Jeong H, Song HN, Kim HJ and Jeong BK: Anticancer effect of benzimidazole derivatives, especially mebendazole, on triple-negative breast cancer (TNBC) and radiotherapy-resistant TNBC in vivo and in vitro. Molecules 26: 5118, 2021.
21. Laudisi F, Marônek M, Di Grazia A, Monteleone G and Stolfi C: Repositioning of anthelmintic drugs for the treatment of cancers of the digestive system. Int J Mol Sci 21: 4957, 2020.
22. Hori A, Imaeda Y, Kubo K and Kusaka M: Novel benzimidazole derivatives selectively inhibit endothelial cell growth and suppress angiogenesis in vitro and in vivo. Cancer Lett 183: 53-60, 2002.
23. Mrkvová Z, Uldrijan S, Pombinho A, Bartůněk P and Slaninová I: Benzimidazoles downregulate Mdm2 and MdmX and activate p53 in MdmX overexpressing tumor cells. Molecules 24: 2152, 2019.
24. Zhang D and Kanakkanthara A: Beyond the paclitaxel and vinca alkaloids: Next generation of plant-derived microtubule-targeting agents with potential anticancer activity. Cancers (Basel) 12: 1721, 2020.
25. Falzone L, Bordonaro R and Libra M: SnapShot: Cancer chemotherapy. Cell 186: 1816-1816.e1, 2023.
26. McGrogan BT, Gilmartin B, Carney DN and McCann A: Taxanes, microtubules and chemoresistant breast cancer. Biochim Biophys Acta 1785: 96-132, 2008.
27. Dhyani P, Quispe C, Sharma E, Bahukhandi A, Sati P, Attri DC, Szopa A, Sharifi-Rad J, Docea AO, Mardare I, *et al*: Anticancer potential of alkaloids: A key emphasis to colchicine, vinblastine, vincristine, vindesine, vinorelbine and vincamine. Cancer Cell Int 22: 206, 2022.
28. Singh R, Bal MS, Singla LD and Kaur P: Detection of anthelmintic resistance in sheep and goat against fenbendazole by faecal egg count reduction test. J Parasit Dis 41: 463-466, 2017.
29. Hennessy DR, Steel JW, Prichard RK and Lacey E: The effect of co-administration of parbendazole on the disposition of oxfendazole in sheep. J Vet Pharmacol Ther 15: 10-18, 1992.
30. Hennessy DR, Lacey E, Prichard RK and Steel JW: Potentiation of the anthelmintic activity of oxfendazole by parbendazole. J Vet Pharmacol Ther 8: 270-275, 1985.
31. Gonzalez AE, Codd EE, Horton J, Garcia HH and Gilman RH: Oxfendazole: A promising agent for the treatment and control of helminth infections in humans. Expert Rev Anti Infect Ther 17: 51-56, 2019.
32. Xu D, Tian W, Jiang C, Huang Z and Zheng S: The anthelmintic agent oxfendazole inhibits cell growth in non-small cell lung cancer by suppressing c-Src activation. Mol Med Rep 19: 2921-2926, 2019.
33. Florio R, Veschi S, Di Giacomo V, Pagotto S, Carradori S, Verginelli F, Cirilli R, Casulli A, Grassadonia A, Tinari N, *et al*: The benzimidazole-based anthelmintic parbendazole: A repurposed drug candidate that synergizes with gemcitabine in pancreatic cancer. Cancers (Basel) 11: 2042, 2019.
34. Libreros S, Garcia-Areas R, Keating P, Gazaniga N, Robinson P, Humbles A and Iragavarapu-Charyulu VL: Allergen induced pulmonary inflammation enhances mammary tumor growth and metastasis: Role of CHI3L1. J Leukoc Biol 97: 929-940, 2015.
35. Cai Y, Zhou J and Webb DC: Treatment of mice with fenbendazole attenuates allergic airways inflammation and Th2 cytokine production in a model of asthma. Immunol Cell Biol 87: 623-629, 2009.
36. Goff SL and Danforth DN: The role of immune cells in breast tissue and immunotherapy for the treatment of breast cancer. Clin Breast Cancer 21: e63-e73, 2021.
37. Libreros S, Garcia-Areas R and Iragavarapu-Charyulu V: CHI3L1 plays a role in cancer through enhanced production of pro-inflammatory/pro-tumorigenic and angiogenic factors. Immunol Res 57: 99-105, 2013.
38. Kim SH, Redvers RP, Chi LH, Ling X, Lucke AJ, Reid RC, Fairlie DP, Martin ACBM, Anderson RL, Denoyer D and Pouliot N: Identification of brain metastasis genes and therapeutic evaluation of histone deacetylase inhibitors in a clinically relevant model of breast cancer brain metastasis. Dis Model Mech 11: DMM034850, 2018.
39. Holliday DL and Speirs V: Choosing the right cell line for breast cancer research. Breast Cancer Res 13: 215, 2011.
40. Kim JB, Urban K, Cochran E, Lee S, Ang A, Rice B, Bata A, Campbell K, Coffee R, Gorodinsky A, *et al*: Non-invasive detection of a small number of bioluminescent cancer cells in vivo. PLoS One 5: e9364, 2010.
41. Erny D, Hrabě de Angelis AL, Jaitin D, Wieghofer P, Staszewski O, David E, Keren-Shaul H, Mahlakoiv T, Jakobshagen K, Buch T, *et al*: Host microbiota constantly control maturation and function of microglia in the CNS. Nat Neurosci 18: 965-977, 2015.
42. Strong P, Clark H and Reid K: Intranasal application of chitin microparticles down-regulates symptoms of allergic hypersensitivity to Dermatophagoides pteronyssinus and Aspergillus fumigatus in murine models of allergy. Clin Exp Allergy 32: 1794-1800, 2002.
43. Nishiyama A, Tsuji S, Yamashita M, Henriksen RA, Myrvik QN and Shibata Y: Phagocytosis of N-acetyl-D-glucosamine particles, a Th1 adjuvant, by RAW 264.7 cells results in MAPK activation and TNF-alpha, but not IL-10, production. Cell Immunol 239: 103-112, 2006.
44. Workman P, Balmain A, Hickman JA, McNally NJ, Rohas AM, Mitchison NA, Pierrepoint CG, Raymond R, Rowlatt C, Stephens TC, *et al*: UKCCCR guidelines for the welfare of animals in experimental neoplasia. Lab Anim 22: 195-201, 1988.
45. Montgomery C: Oncologic and toxicologic research: Alleviation and control of pain and distress in laboratory animals. Cancer Bull 42: 230-237, 1990.
46. Ullman-Culleré MH and Foltz CJ: Body condition scoring: A rapid and accurate method for assessing health status in mice. Lab Anim Sci 49: 319-323, 1999.
47. Isgor C and Watson SJ: Estrogen receptor alpha and beta mRNA expressions by proliferating and differentiating cells in the adult rat dentate gyrus and subventricular zone. Neuroscience 134: 847-856, 2005.
48. Shihan MH, Novo SG, Le Marchand SJ, Wang Y and Duncan MK: A simple method for quantitating confocal fluorescent images. Biochem Biophys Rep 25: 100916, 2021.
49. Han J, Lin K, Sequeira C and Borchers CH: An isotope-labeled chemical derivatization method for the quantitation of short-chain fatty acids in human feces by liquid chromatography-tandem mass spectrometry. Anal Chim Acta 854: 86-94, 2015.
50. Saha S, Day-Walsh P, Shehata E and Kroon PA: Development and validation of a LC-MS/MS technique for the analysis of short chain fatty acids in tissues and biological fluids without derivatisation using isotope labelled internal standards. Molecules 26: 6444, 2021. https://doi.org/10.3390/molecules26216444.
51. Nagatomo R, Kaneko H, Kamatsuki S, Ichimura-Shimizu M, Ishimaru N, Tsuneyama K and Inoue K: Short-chain fatty acids profiling in biological samples from a mouse model of Sjögren's syndrome based on derivatized LC-MS/MS assay. J Chromatogr B Analyt Technol Biomed Life Sci 1210: 123432, 2022.
52. Guzmán EA, Pitts TP, Winder PL and Wright AE: The marine natural product furospinulosin 1 induces apoptosis in MDA-MB-231 triple negative breast cancer cell spheroids, but not in cells grown traditionally with longer treatment. Mar Drugs 19: 249, 2021.
53. Das GC, Holiday D, Gallardo R and Haas C: Taxol-induced cell cycle arrest and apoptosis: Dose-response relationship in lung cancer cells of different wild-type p53 status and under isogenic condition. Cancer Lett 165: 147-153, 2001.
54. Mikhail AS, Eetezadi S and Allen C: Multicellular tumor spheroids for evaluation of cytotoxicity and tumor growth inhibitory effects of nanomedicines in vitro: A comparison of docetaxel-loaded block copolymer micelles and Taxotere®. PLoS One 8: e62630, 2013.
55. Adcock AF, Trivedi G, Edmondson R, Spearman C and Yang L: Three-dimensional (3D) cell cultures in cell-based assays for in-vitro evaluation of anticancer drugs. J Anal Bioanal Tech 6: 247, 2015.
56. Sazonova EV, Kopeina GS, Imyanitov EN and Zhivotovsky B: Platinum drugs and taxanes: Can we overcome resistance? Cell Death Discov 7: 155, 2021.
57. Mann J, Yang N, Montpetit R, Kirschenman R, Lemieux H and Goping IS: BAD sensitizes breast cancer cells to docetaxel with increased mitotic arrest and necroptosis. Sci Rep 10: 355, 2020.
58. Wang TH, Wang HS and Soong YK: Paclitaxel-induced cell death: Where the cell cycle and apoptosis come together. Cancer 88: 2619-2628, 2000.
59. Yang G, Chen S, Deng B, Tan C, Deng J, Zhu G, Yin Y and Ren W: Implication of G protein-coupled receptor 43 in intestinal inflammation: A mini-review. Front Immunol 9:1434, 2018.

60. Spagnuolo PA, Hu J, Hurren R, Wang X, Gronda M, Sukhai MA, Di Meo A, Boss J, Ashali I, Beheshti Zavareh R, *et al*: The antihelmintic flubendazole inhibits microtubule function through a mechanism distinct from vinca alkaloids and displays preclinical activity in leukemia and myeloma. Blood 115: 4824-4833, 2010.
61. Furtado LFV, de Paiva Bello ACP and Rabelo ÉML: Benzimidazole resistance in helminths: From problem to diagnosis. Acta Trop 162: 95-102, 2016.
62. Moudi M, Go R, Yien CYS and Nazre M: Vinca alkaloids. Int J Prev Med 4: 1231-1235, 2013.
63. Zhou J and Giannakakou P: Targeting microtubules for cancer chemotherapy. Curr Med Chem Anticancer Agents 5: 65-71, 2005.
64. Redman E, Whitelaw F, Tait A, Burgess C, Bartley Y, Skuce PJ, Jackson F and Gilleard JS: The emergence of resistance to the benzimidazole anthlemintics in parasitic nematodes of livestock is characterised by multiple independent hard and soft selective sweeps. PLoS Negl Trop Dis 9: e0003494, 2015.
65. Lv Y, Ma X, Du Y and Feng J: Understanding patterns of brain metastasis in triple-negative breast cancer and exploring potential therapeutic targets. Onco Targets Ther 14: 589-607, 2021.
66. Syriac AK, Nandu NS and Leone JP: Central nervous system metastases from triple-negative breast cancer: Current treatments and future prospective. Breast Cancer (Dove Med Press) 14: 1-13, 2022.
67. Dogra N, Kumar A and Mukhopadhyay T: Fenbendazole acts as a moderate microtubule destabilizing agent and causes cancer cell death by modulating multiple cellular pathways. Sci Rep 8: 11926, 2018.
68. Mirzaei R, Afaghi A, Babakhani S, Sohrabi MR, Hosseini-Fard SR, Babolhavaeji K, Khani Ali Akbari S, Yousefimashouf R and Karampoor S: Role of microbiota-derived short-chain fatty acids in cancer development and prevention. Biomed Pharmacother 139: 111619, 2021.
69. Feitelson MA, Arzumanyan A, Medhat A and Spector I: Short-chain fatty acids in cancer pathogenesis. Cancer Metastasis Rev 42: 677-698, 2023.
70. Dutta J, Tripathi S and Dutta PK: Progress in antimicrobial activities of chitin, chitosan and its oligosaccharides: A systematic study needs for food applications. Food Sci Technol Int 18: 3-34, 2012.
71. Nagatani K, Wang S, Llado V, Lau CW, Li Z, Mizoguchi A, Nagler CR, Shibata Y, Reinecker HC, Mora JR and Mizoguchi E: Chitin microparticles for the control of intestinal inflammation. Inflamm Bowel Dis 18: 1698-1710, 2012.
72. Tedelind S, Westberg F, Kjerrulf M and Vidal A: Anti-inflammatory properties of the short-chain fatty acids acetate and propionate: A study with relevance to inflammatory bowel disease. World J Gastroenterol 13: 2826-2832, 2007.
73. Liu Q, Tian X, Maruyama D, Arjomandi M and Prakash A: Lung immune tone via gut-lung axis: Gut-derived LPS and short-chain fatty acids' immunometabolic regulation of lung IL-1β, FFAR2 and FFAR3 expression. Am J Physiol Lung Cell Mol Physiol 321: L65-L68, 2021.
74. Logsdon AF, Erickson MA, Rhea EM, Salameh TS and Banks WA: Gut reactions: How the blood-brain barrier connects the microbiome and the brain. Exp Biol Med (Maywood) 243: 159-165, 2018.
75. Hirschhaeuser F, Menne H, Dittfeld C, West J, Mueller-Klieser W and Kunz-Schughart LA: Multicellular tumor spheroids: An underestimated tool is catching up again. J Biotechnol 148: 3-15, 2010.
76. Edmondson R, Broglie JJ, Adcock AF and Yang L: Three-dimensional cell culture systems and their applications in drug discovery and cell-based biosensors. Assay Drug Dev Technol 12: 207-218, 2014.
77. Riedl A, Schlederer M, Pudelko K, Stadler M, Walter S, Unterleuthner D, Unger C, Kramer N, Hengstschläger M, Kenner L, *et al*: Comparison of cancer cells in 2D vs 3D culture reveals differences in AKT-mTOR-S6K signaling and drug responses. J Cell Sci 130: 203-218, 2017.
78. Rahimifard M, Bagheri Z, Hadjighassem M, Jaktaji RP, Behroodi E, Haghi-Aminjan H, Movahed MA, Latifi H, Hosseindoost S, Zarghi A and Pourahmad J: Investigation of anti-cancer effects of new pyrazino[1,2-a]benzimidazole derivatives on human glioblastoma cells through 2D in vitro model and 3D-printed microfluidic device. Life Sci 302: 120505, 2022.
79. Zhang X, Zhao J, Gao X, Pei D and Gao C: Anthelmintic drug albendazole arrests human gastric cancer cells at the mitotic phase and induces apoptosis. Exp Ther Med 13: 595-603, 2017.
80. Liu H, Sun H, Zhang B, Liu S, Deng S, Weng Z, Zuo B, Yang J and He Y: ^{18}F-FDG PET imaging for monitoring the early anti-tumor effect of albendazole on triple-negative breast cancer. Breast Cancer 27: 372-380, 2020.
81. Dogra N and Mukhopadhyay T: Impairment of the ubiquitin-proteasomepathwaybymethylN-(6-phenylsulfanyl-1H-benzimidazol-2-yl) carbamate leads to a potent cytotoxic effect in tumor cells: A novel antiproliferative agent with a potential therapeutic implication. J Biol Chem 287: 30625-30640, 2012.
82. Pinto LC, Mesquita FP, Soares BM, da Silva EL, Puty B, de Oliveira EHC, Burbano RR and Montenegro RC: Mebendazole induces apoptosis via C-MYC inactivation in malignant ascites cell line (AGP01). Toxicol In Vitro 60: 305-312, 2019.
83. Chen Q, Li Y, Zhou X and Li R: Oxibendazole inhibits prostate cancer cell growth. Oncol Lett 15: 2218-2226, 2018.
84. Zhou F, Du J and Wang J: Albendazole inhibits HIF-1α-dependent glycolysis and VEGF expression in non-small cell lung cancer cells. Mol Cell Biochem 428: 171-178, 2017.
85. Sung SJ, Kim HK, Hong YK and Joe YA: Autophagy is a potential target for enhancing the anti-angiogenic effect of mebendazole in endothelial cells. Biomol Ther (Seoul) 27: 117-125, 2019.
86. Kralova V, Hanušová V, Caltová K, Špaček P, Hochmalová M, Skálová L and Rudolf E: Flubendazole and mebendazole impair migration and epithelial to mesenchymal transition in oral cell lines. Chem Biol Interact 293: 124-132, 2018.